

RESEARCH ARTICLE

Vision in avian emberizid foragers: maximizing both binocular vision and fronto-lateral visual acuity

Bret A. Moore, Diana Pita, Luke P. Tyrrell and Esteban Fernández-Juricic*

ABSTRACT

Avian species vary in their visual system configuration, but previous studies have often compared single visual traits between two to three distantly related species. However, birds use different visual dimensions that cannot be maximized simultaneously to meet different perceptual demands, potentially leading to trade-offs between visual traits. We studied the degree of inter-specific variation in multiple visual traits related to foraging and anti-predator behaviors in nine species of closely related emberizid sparrows, controlling for phylogenetic effects. Emberizid sparrows maximize binocular vision, even seeing their bill tips in some eye positions, which may enhance the detection of prey and facilitate food handling. Sparrows have a single retinal center of acute vision (i.e. fovea) projecting fronto-laterally (but not into the binocular field). The foveal projection close to the edge of the binocular field may shorten the time to gather and process both monocular and binocular visual information from the foraging substrate. Contrary to previous work, we found that species with larger visual fields had higher visual acuity, which may compensate for larger blind spots (i.e. pectens) above the center of acute vision, enhancing predator detection. Finally, species with a steeper change in ganglion cell density across the retina had higher eye movement amplitude, probably due to a more pronounced reduction in visual resolution away from the fovea, which would need to be moved around more frequently. The visual configuration of emberizid passive prey foragers is substantially different from that of previously studied avian groups (e.g. sit-and-wait and tactile foragers).

KEY WORDS: Birds, Visual acuity, Visual fields

INTRODUCTION

The question of how birds see their world has been the subject of considerable attention (e.g. Walls, 1942), partly because the properties of the avian visual system are different from that of humans (e.g. wider visual spectrum, higher temporal visual resolution etc.; Cuthill, 2006). Understanding how birds gather different types of information from the environment can help us explain multiple behaviors that have been studied over decades (Birkhead, 2012). This is relevant because birds have often been used as model systems to address fundamental questions in evolutionary ecology (Birkhead et al., 2014).

Interestingly, the avian visual system varies considerably between species in terms of visual acuity (Kiltie, 2000), type and position of the centers of acute vision (e.g. fovea, area, visual streak; Meyer, 1977; Hughes, 1977; Moore et al., 2012) and visual field configuration

(Martin, 2007). This inter-specific variability has generally been studied from a unidimensional perspective (i.e. variation in the size of the binocular field or visual acuity or placement of the orbits). However, this approach does not take into account the fact that birds deal with multiple types of visual information simultaneously. For instance, visual acuity is used to detect predators and binocular vision is used to guide the bill towards food (Martin, 2014). By studying different visual dimensions, particularly in closely related species, we can begin to understand the steps involved in the evolutionary divergence of the avian visual system (Martin, 2012) as well as the role of sensory specializations in gathering specific types of visual information that can be the basis of partitioning foraging resources within ecological niches (Martin and Prince, 2001; Siemers and Swift, 2006; Safi and Siemers, 2010).

Active prey foragers that employ sit-and-wait foraging tactics, including diurnal raptors (Reymond, 1985; Frost et al., 1990; Inzunza et al., 1991; O'Rourke et al., 2010a) and flycatchers (Moroney and Pettigrew, 1987; Coimbra et al., 2006, 2009; Gall and Fernández-Juricic, 2010), have very specialized visual systems. Their retinae have two centers of acute vision: one projects into the lateral visual field to detect prey at far distances, while the other projects into the binocular field to grab prey at close distances (Tucker, 2000). Sit-and-wait foragers also tend to have relatively high visual acuity, wide blind areas and a low degree of eye movements (Jones et al., 2007; O'Rourke et al., 2010a).

The visual system of passive prey foragers, which both detect and grab prey items at close distances (i.e. ground and tree foragers), has been studied on model species from different Orders (pigeons, chickens, budgerigars and some songbirds; e.g. Lazareva et al., 2012). However, we know little about the degree of between-species variation within taxonomic groups (Order or Family). Songbirds (i.e. Order Passeriformes) that are passive prey foragers appear to share some visual traits (Fernández-Juricic et al., 2008; Dolan and Fernández-Juricic, 2010; Moore et al., 2013): (1) a single retinal center of acute vision (i.e. fovea) projecting into the lateral field; (2) relatively wide binocular fields; (3) the bill projecting towards (but not intruding into) the binocular field; and (4) a large degree of eye movements that allows for varying the size of the binocular field and blind area through eye convergence and divergence. However, it is challenging to make generalizations on the visual system of these songbirds for three main reasons. First, studies have often included species that are phylogenetically very distant; hence, functional interpretations on the visual system configuration are confounded by phylogenetic variation in morphology and behavior (Martin, 2014). Second, many studies looking at between-species variation in visual traits include too few species (often 2–3) and fail to control for phylogenetic effects (Martin, 2014). Third, songbirds have a large diversity in morphology, diet and behavior (Ricklefs, 2012), which is expected to be mirrored in their visual systems to enhance visual performance in different habitat types (Boughman, 2002; Seehausen et al., 2008; Dalton et al., 2010).

Department of Biological Sciences, Purdue University, 915 W. State Street, West Lafayette, IN 47907, USA.

*Author for correspondence (efernan@purdue.edu)

In this study, we assessed the degree of inter-specific variation in several key visual dimensions related to foraging and anti-predator behaviors and tested specific predictions about their co-variation in species belonging to the Emberizidae family (Order Passeriformes). Emberizid sparrows forage close to the ground on seeds during the winter and insects during the breeding season and escape to vegetative cover when attacked by aerial and ground predators (Elphick et al., 2001). The over-reaching hypothesis behind our predictions (see below) is that different visual dimensions cannot be maximized simultaneously to meet different perceptual demands (Martin, 2014). Consequently, ours is the first study taking into account multiple visual dimensions from a quantitative perspective and testing for trade-offs in avian visual configuration.

Our study is divided in two parts. First, we established the degree of inter-specific variability in four visual dimensions in seven species of closely related emberizids: American tree sparrow *Spizella arborea* Wilson 1810, chipping sparrow *Spizella passerine* Bechstein 1798, dark-eyed junco *Junco hyemalis* Linnaeus 1758, Eastern towhee *Pipilo erythrophthalmus* Linnaeus 1758, field sparrow *Spizella pusilla* Wilson 1810, song sparrow *Melospiza melodia* Wilson 1810 and white-throated sparrow *Zonotrichia albicollis* Gmelin 1789 (supplementary material Table S1). We studied: (1) eye size and retinal ganglion cell density (i.e. cells that transfer information from the retina to the visual centers of the brain) as proxies of visual acuity; (2) ganglion cell density profiles across the retina as proxies of the position of the center of acute vision and its projection into the visual field, which is usually associated with visual attention (Bisley, 2011); (3) visual field configuration as a proxy of visual coverage around the head (i.e. size of the binocular and lateral fields, and blind area); and (4) degree of eye movement as a proxy of the extent to which the center of acute vision can be moved around the visual space for scanning purposes. Additionally, we measured bill size (length, width, depth) to assess its influence on the configuration of the visual field. Second, we tested specific predictions considering these seven emberizid species along with two others belonging to the same Family already described in the literature (California towhee *Pipilo crissalis* and white-crowned sparrow *Zonotrichia leucophrys*; Fernández-Juricic et al., 2011a; supplementary material Table S1). We studied the following relationships between visual dimensions in the context of foraging and anti-predator behaviors, controlling for the degree of phylogenetic relatedness among the nine species.

Binocular field width and bill size

Martin (2009) proposed that binocular vision in birds is mostly associated with controlling bill direction and time of contact with targets. Therefore, species that guide their bills to explore the substrate and glean food items are expected to have relatively wider binocular fields (Martin, 2014). In Passeriformes, the bill usually projects towards the binocular field (e.g. Tyrrell et al., 2013; Baumhardt et al., 2014). The implication is that larger bills can block areas of binocular overlap leaving them covered only by monocular vision (i.e. the visual field of a single eye; Moore et al., 2013). Therefore, species with more frontally placed eyes would not necessarily gain the full benefit of increased binocular vision due to obstruction by the bill. This shadowing effect would be more pronounced in species with larger bills. Therefore, we predicted that species with larger bills would have narrower binocular fields.

Pecten size, binocular field width and degree of eye movement

Birds have a pecten, which is a pigmented vascular structure that supplies nutrients to the avian retina but reduces visual coverage

because its projection generates a blind spot in the upper part of the visual field, right above the fovea (Meyer, 1977; van den Hout and Martin, 2011). The pecten has been hypothesized to be involved in reducing glare within the eye chamber (Barlow and Ostwald, 1972), enhancing the detection of moving images (Crozier and Wolf, 1944), stabilizing the vitreous humor (Tucker, 1975) and supplying oxygen to the retina (Pettigrew et al., 1990). The size of the pecten varies substantially between species (Wood, 1917; Meyer, 1977). Given that the pecten projects towards the edges of the binocular field (see below), larger pectens could constrain the space available for binocular vision. This would lead to a negative relationship between the size of the projection of the pecten and the binocular field width with the eyes at rest. If emberizid sparrows need to maximize the size of the binocular field for foraging purposes, one strategy is to converge their eyes when looking for and gleaning food to enhance binocular vision. Thus, we predicted that species with larger pectens would have higher degrees of eye movement, compared with those with smaller pectens, to compensate for narrower binocular fields with the eyes at rest.

Blind spots and eye size

High levels of ambient light can decrease visual performance (i.e. reduce image contrast) because of light scattering within the eye chamber (i.e. glare effects; Koch, 1989). Species with larger eyes can be more prone to glare effects because of larger optical apertures leading to a greater influx of sunlight (Martin and Katzir, 2000). Positioning the sun's image in any blind spot (i.e. blind area, pecten) would reduce glare effects, which leads to two alternative solutions for species with larger eyes: larger blind areas (Martin and Katzir, 2000) and/or larger pectens (Fernández-Juricic and Tran, 2007; van den Hout and Martin, 2011). We thus predicted a positive association between eye size and pecten size, as well as eye size and blind area width.

Visual coverage and visual acuity

One of the implications of the predicted positive association between eye size and blind area width is that visual acuity (i.e. a positive function of eye size and ganglion cell density; Pettigrew et al., 1988) and visual coverage (i.e. the inverse of the blind area; Martin, 2014) may be related. Additionally, species with lower visual acuity have been proposed to compensate for the limitations of detecting predators from far distances by having more laterally placed eyes to enhance the chances of detection from a wider area around their heads (Hughes, 1977). Consequently, we predicted that species with lower visual acuity would have wider visual coverage.

Retinal configuration and degree of eye movements

The density of ganglion cells (and thus visual acuity) varies across the vertebrate retina (Collin, 1999), being higher close to center of acute vision than the retinal periphery in many songbirds (e.g. Moore et al., 2013; Tyrrell et al., 2013). Species with lower ganglion cell density, hence lower acuity, in the retinal periphery compared with the retinal center have been proposed to rely more on the high visual acuity provided by the center of acute vision (Dolan and Fernández-Juricic, 2010). This would increase the need for a higher degree of eye movement to move the center of acute vision around and sample the visual environment with high visual resolution (Fernández-Juricic et al., 2011a). Therefore, we predicted that species with a more pronounced difference in cell density across the retina would have a higher degree of eye movement.

RESULTS

We found a large degree of interspecific variation in most of the visual traits studied. We first provide a quantitative account of this

Table 1. Least-squares means of different visual traits of seven emberizid sparrows

	American tree sparrow	Chipping sparrow	Dark-eyed junco	Eastern towhee	Field sparrow	Song sparrow	White-throated sparrow
Axial length (mm)	6.08±0.07	5.37±0.08	6.23±0.07	7.59±0.11	5.63±0.07	6.53±0.07	7.06±0.08
x-coordinate	-0.082±0.040	-0.231±0.040	-0.143±0.035	-0.118±0.049	-0.116±0.035	-0.154±0.040	-0.245±0.049
x-coordinate 95% CI	-0.168 to 0.005	-0.317 to -0.145	-0.218 to -0.068	-0.223 to -0.012	-0.191 to -0.042	-0.240 to -0.068	-0.350 to -0.139
y-coordinate	0.100±0.051	0.069±0.051	0.107±0.044	0.106±0.062	0.134±0.044	-0.002±0.051	0.148±0.062
y-coordinate 95% CI	-0.009–0.209	-0.040–0.179	0.013–0.202	-0.028–0.240	0.039–0.228	-0.111–0.108	0.014–0.282
Nasal slope	3.693±0.368	3.890±0.450	2.458±0.319	3.065±0.450	4.327±0.368	2.727±0.368	3.130±0.450
Temporal slope	5.227±0.542	5.505±0.664	3.095±0.469	5.590±0.664	4.973±0.542	4.313±0.542	6.365±0.664
Dorsal slope	6.770±0.556	6.040±0.681	3.805±0.481	4.240±0.681	6.780±0.556	3.930±0.556	5.645±0.681
Ventral slope	4.477±0.382	5.050±0.468	3.538±0.331	4.465±0.468	4.477±0.382	3.660±0.382	3.550±0.468
Overall RGC density (cells mm ⁻²)	23,423±297	22,570±321	18,098±296	17,882±443	19,801±283	18,338±288	19,094±322
Highest RGC density (cells mm ⁻²)	42,319±1361	47,920±1522	34,938±1361	38,188±2152	41,765±1361	37,046±1361	37,557±1522
Visual acuity (cycles/deg)	7.03	6.62	6.55	8.35	6.45	7.07	7.70
Binocular field across elevations (deg)	24.64±0.72	24.03±0.78	24.55±0.56	23.41±0.87	25.27±0.65	24.50±0.55	26.42±0.51
Blind area across elevations (deg)	20.38±1.10	26.73±1.03	17.30±0.89	24.39±1.73	27.13±0.99	21.19±0.97	16.77±0.97
Eye movement across elevations (deg)	21.81±0.53	31.44±0.59	32.95±0.39	35.26±0.55	35.94±0.51	32.80±0.41	30.81±0.34
Pecten width across elevations (deg)	14.55±0.96	19.63±0.93	24.46±0.73	26.96±1.38	23.78±0.76	24.25±0.74	22.69±0.73
Max distance to resolve Cooper's hawks (m)	306	288	285	364	281	308	335
Max distance to resolve sharp-shinned hawks (m)	199	188	186	237	183	201	218

Coordinates (x, y) represent the position of the fovea in the retina and slopes indicate the degree of variation in ganglion cell density from the retinal periphery to the fovea. See text for further details. Values are means±s.e. CI, confidence interval; RGC, retinal ganglion cell.

variability in the seven species of emberizid sparrows studied for the first time here (Table 1). We then establish the associations between different visual traits including these seven species along with two other emberizid sparrows studied before (Fernández-Juricic et al., 2011a).

Eye size, retinal ganglion cell density and visual acuity

Eye axial length varied significantly among species ($F_{6,43}=79.40$, $P<0.001$), from 5.37 mm (chipping sparrow) to 7.59 mm (Eastern towhee; Table 1). Pooling all species, the relationship between (\log_{10}) axial length and (\log_{10}) body mass was significant ($F_{1,46}=129.29$, $P<0.001$; adjusted $R^2=0.74$). The residuals of this relationship (i.e. eye axial length relative to body mass) differed significantly among species ($F_{6,41}=5.59$, $P<0.001$). Three species showed smaller eyes relative to their body mass: chipping sparrow, -0.0209 ± 0.0072 ; American tree sparrow, -0.0113 ± 0.0062 ; and dark-eyed junco, -0.0109 ± 0.0058 . Four species showed larger eyes relative to their body mass: white-throated sparrow, 0.0223 ± 0.0079 ;

song sparrow, 0.0194 ± 0.0062 ; field sparrow, 0.0051 ± 0.0058 ; and Eastern towhee, 0.0004 ± 0.0102 .

The mean overall density of retinal ganglion cells differed significantly among species ($F_{6,23}=51.97$, $P<0.001$), from 23,423 cells mm⁻² (American tree sparrow) to 17,882 cells mm⁻² (Eastern towhee; Table 1). The highest ganglion cell density (in the quadrats around the center of acute vision) also varied significantly among species ($F_{6,23}=8.91$, $P<0.001$), from 34,938 cells mm⁻² (dark-eyed junco) to 47,920 cells mm⁻² (chipping sparrow; Table 1).

Based on the averaged eye axial length and highest density of ganglion cells, we found that visual acuity varied by about 25% among emberizid sparrows (Table 1). Based on their visual acuities, we estimated the maximum distances at which each emberizid species would be able to resolve two of their most common predators under optimal ambient light conditions (Table 1). For the Cooper's hawk, the maximum distance varied from 281 to 364 m and for the Sharp-shinned hawk, from 183 to 237 m (Table 1).

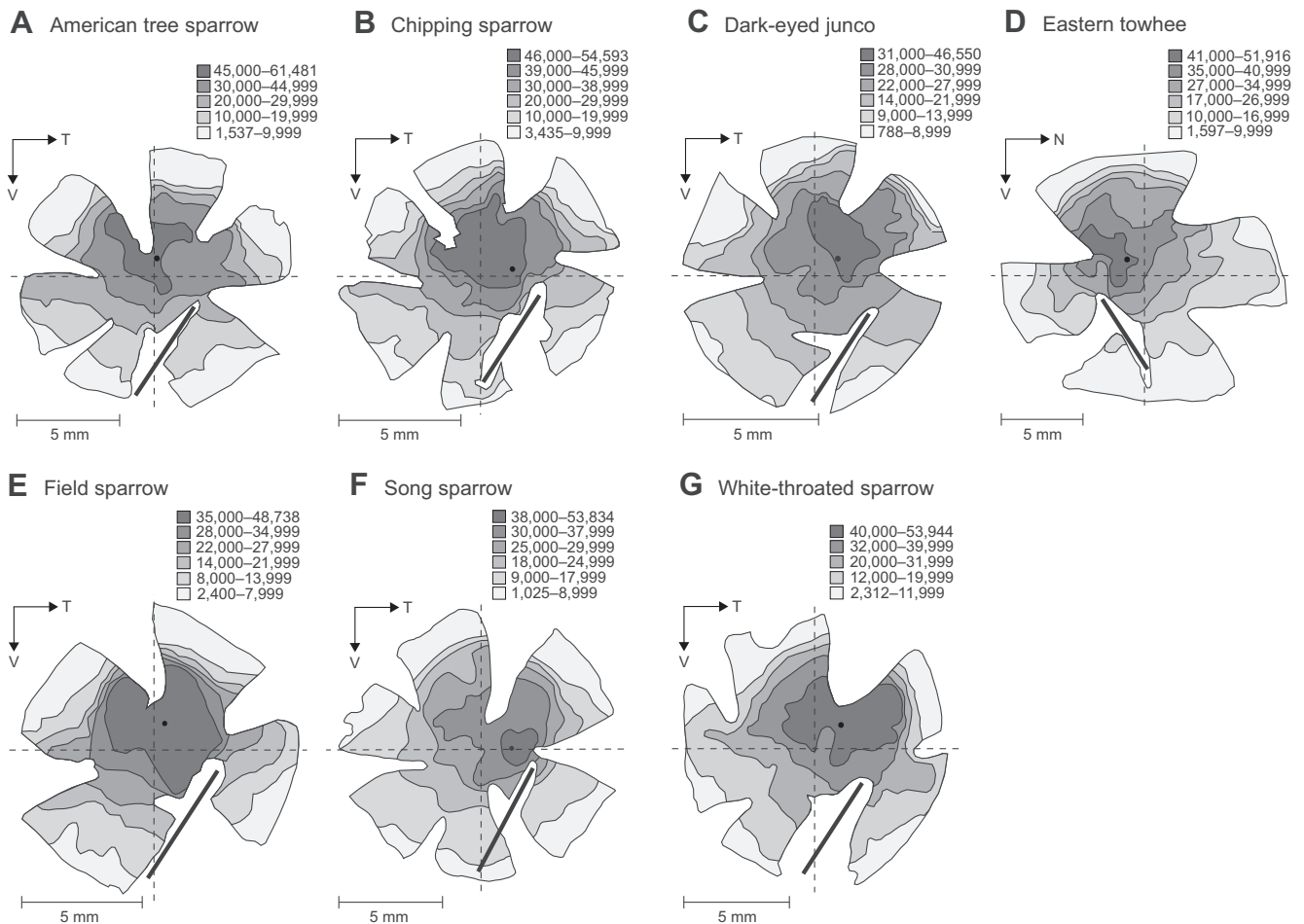


Fig. 1. Topographic maps of retinal ganglion cell densities of seven emberizid sparrows. (A) American tree sparrow, (B) chipping sparrow, (C) dark-eyed junco, (D) Eastern towhee, (E) field sparrow, (F) song sparrow and (G) white-throated sparrow. Numbers represent ranges of cell densities in cells mm^{-2} . The dashed lines represent the nasal-temporal and dorsal-ventral axes, with the intersection of the two axes indicating the center of the retina. The fovea is indicated by the black dot in each map and the pecten is indicated by the thick black bar. All maps are of left eyes except for D. V, ventral; T, temporal; N, nasal.

Retinal configuration

Fig. 1 shows a representative topographic map of the distribution of ganglion cells for each of the studied species. These maps show a concentric increase in ganglion cell density from the periphery to an approximate central location in the retina (black dots in Fig. 1). Based on morphological features on the whole-mount (i.e. small circular area devoid of retinal ganglion cells at the very center, but surrounded by the highest ganglion cell density), we determined that all the studied species appear to have a single fovea per retina. To corroborate this, we adjusted the microscope focus (achieving a $\times 400$ magnification through a $\times 40$ objective lens and a $\times 10$ ocular lens) and observed changes in the surface of the retinal tissue that suggested a potential invagination characteristic of a fovea. Based on tissue availability, we also cut cross-sections for some of the studied species (song sparrow, dark-eyed junco, field sparrow) and confirmed that the morphological characteristics observed on the whole-mounted tissue corresponded to a fovea (i.e. invagination of the ganglion cell and inner nuclear layers; photographs available upon request).

Based on the x -coordinates of the fovea position of all species (Table 1), the single fovea was located slightly off center towards the temporal side of the retina (Fig. 1). We estimated the 95% confidence intervals of the coordinates to determine the likelihood of the fovea being off the retinal center for each species. Based on

the negative upper and lower bound 95% confidence intervals of the fovea x -coordinates (Table 1), the temporal displacement of the fovea was prevalent in chipping sparrows, dark-eyed juncos, Eastern towhees, field sparrows, song sparrows and white-throated sparrows. However, the 95% confidence intervals of the fovea x -coordinate of American tree sparrows included positive values, which suggests that in this species the temporal placement of the fovea cannot be discriminated from a central placement.

The y -coordinates of the fovea position in the dorso-ventral axis are presented in Table 1. Based on the positive upper and lower bound 95% confidence intervals of these y -coordinates (Table 1), dark-eyed juncos, field sparrows and white-throated sparrows appeared to have their foveae displaced dorsally in relation to the center of the retina (Fig. 1). However, the positive upper and negative lower bound 95% confidence intervals of the fovea y -coordinate of American tree sparrows, chipping sparrows, Eastern towhees and song sparrows (Table 1) suggest that the dorsal or ventral placement of the fovea cannot be discriminated from a central placement.

American tree sparrows have an approximately central fovea; dark-eyed juncos, field sparrows and white-throated sparrows have a dorso-temporal fovea, and chipping sparrows, Eastern towhees and song sparrows a centro-temporal fovea. Under the assumptions explained in the Materials and methods, we estimated the

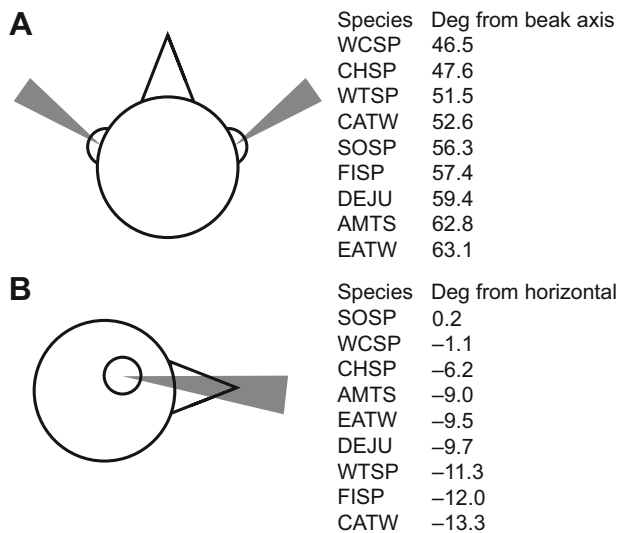


Fig. 2. Schematic representations of the approximate angular projections of the foveae into the visual field while the eyes are in a resting position. (A) Top view. The front edge of the gray triangles represents the furthest forward projection (white-crowned sparrow) and the back edge represents the least forward projection (Eastern towhee). All other species fall within the gray zone. (B) Side view. The top edge of the gray triangle represents the most horizontal fovea projection (song sparrow) and the bottom edge represents the most downward fovea projection (California towhee). All other species fall within the gray zone. Negative numbers denote downward projections. AMTS, American tree sparrow; CATW, California towhee; CHSP, Chipping sparrow; DEJU, Dark-eyed junco; EATW, Eastern towhee; FISP, Field sparrow; SOSP, Song sparrow; WCSP, White-crowned sparrow; WTSP, White-throated sparrow.

approximate projection of the fovea from top and side views using the averaged values of the x - and y -coordinates (Fig. 2). In general, based on the 95% confidence intervals, the fovea projects fronto-laterally in all species (Fig. 2A). From a side view, the fovea tends to project below the bill in dark-eyed juncos, field sparrows and white-throated sparrows, but in the other species the foveal projection appears as straight-ahead (Fig. 2B; supplementary material Fig. S1).

We found significant variation among species in the nasal ($F_{6,12}=3.41$, $P=0.033$), temporal ($F_{6,12}=3.80$, $P=0.023$) and dorsal ($F_{6,12}=5.60$, $P=0.006$) slopes of ganglion cell density change between the retinal periphery and the fovea. In general, dark-eyed juncos and song sparrows had the lowest values in the three slopes, suggesting a shallow change in ganglion cell density (and hence spatial visual resolution) across the retina (Table 1). We did not find significant differences among species in the ventral slope values ($F_{6,12}=2.04$, $P=0.137$).

Visual field configuration and degree of eye movement

At the horizontal plane with the eyes at rest, the width of the binocular field varied by 29% among species (from 33 deg in the Eastern towhee to 44 deg in the chipping sparrow, supplementary material Fig. S2). Across all recorded elevations, we found significant differences in the width of the binocular field among species (species, $F_{6,43}=3.41$, $P=0.007$; elevation, $F_{19,665}=133.62$, $P<0.001$; Fig. 3, supplementary material Fig. S3), with white-throated sparrows having the highest values (Table 1). At the horizontal plane with the eyes at rest, the width of the blind area varied by 48% among species (from 31 deg in the dark-eyed junco to 46 deg in the field sparrow; supplementary material Fig. S2). Taking into account all recorded elevations, the width of the blind area differed significantly among species (species, $F_{6,43}=24.53$,

$P<0.001$; elevation, $F_{10,322}=61.55$, $P<0.001$; supplementary material Fig. S3), from 17 deg in the white-throated sparrow to 27 deg in the field sparrow (Table 1).

Across all recorded elevations, the degree of eye movement varied significantly among species (species, $F_{6,43}=24.53$, $P<0.001$; elevation, $F_{10,322}=61.55$, $P<0.001$; supplementary material Fig. S4) by 48% (from 22 deg in the American tree sparrow to 36 deg in the field sparrow; Table 1). The differential ability to move the eyes changed the configuration of the visual fields of each of the species when the eyes were either converged or diverged. When the eyes converged, the width of the binocular field increased substantially along the horizontal plane, varying by 26% (from 53 deg in the American tree sparrow to 69 deg in the Eastern towhee; supplementary material Fig. S5). In all species but one (American tree sparrow) individuals converged their eyes to a degree that they could see their bill tips, but only in the converged eye position (supplementary material Fig. S6). When the eyes diverged, visual coverage increased in all species due to a reduction in the width of the blind area, which varied by 179% along the horizontal plane (from 1 deg in the chipping and field sparrows to 18 deg in the American tree sparrow).

Finally, the width of the projection of the pecten (i.e. blind spot in the upper and frontal part of the visual field) across all measured elevations with the eyes at rest varied significantly between species ($F_{6,36}=18.01$, $P<0.001$; elevation, $F_{7,228}=60.68$, $P<0.001$, Fig. 3) by 57% (from 15 deg in the American tree sparrow to 27 deg in the Eastern towhee; Table 1).

Binocular field width and bill size

Supplementary material Table S2 reports the degree of inter-specific variation in bill size. We found that there was no significant association between the bill size and the width of the binocular field with the eyes at rest ($F_{2,7}=0.95$, $P=0.432$, $R^2=0.12$, coefficient 1.34 ± 1.37 , $\lambda=0$) and with the eyes converged ($F_{2,7}=0.23$, $P=0.793$, $R^2=0.03$, coefficient 1.58 ± 3.23 , $\lambda=0$) at the plane of the bill.

Pecten size, binocular field width and degree of eye movement

As predicted, we found a negative association between pecten size across all elevations and binocular field width with the eyes at rest at the plane of the bill ($F_{2,7}=7.34$, $P=0.019$, $R^2=0.51$, coefficient -0.70 ± 0.26 , $\lambda=0$). Thus, species with wider pecten projections tended to have narrower binocular fields (Fig. 4A). This prediction assumes a negative association between the width of the binocular field with the eyes at rest and the width of the binocular field with the eyes converged at the plane of the bill, which was significant ($F_{2,7}=9.76$, $P=0.009$, $R^2=0.58$, coefficient -1.71 ± 0.55 , $\lambda=0$). Species with wider binocular fields with the eyes at rest tended to converge their eyes less into the binocular field (Fig. 4B).

We also found support for the second prediction: a significant and positive association between the width of the pecten across all elevations and the degree of eye movement across all elevations ($F_{2,7}=9.09$, $P=0.011$, $R^2=0.56$, coefficient 1.89 ± 0.63 , $\lambda=0$). Thus, species with wider pectens tended to move their eyes more (Fig. 4C).

Blind spots and eye size

We found no significant association between the width of the blind area across all elevations with the eyes at rest and (\log_{10}) eye axial length ($F_{2,7}=1.89$, $P=0.219$, $R^2=0.21$, coefficient -29.45 ± 21.38 , $\lambda=0$). Similarly, the width of the pecten across all elevations was not significantly associated with (\log_{10}) eye axial length ($F_{2,7}=0.06$, $P=0.945$, $R^2=0.01$, coefficient 5.72 ± 23.96 , $\lambda=0$).

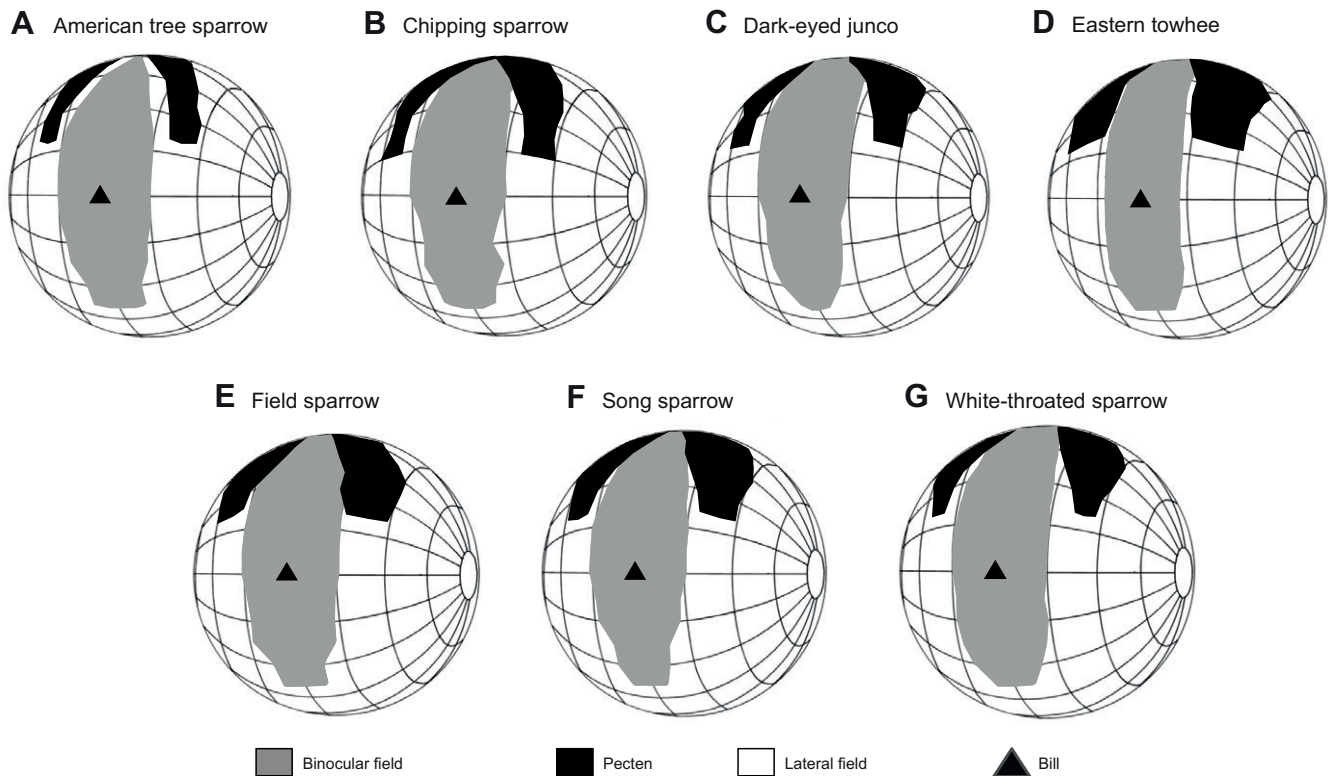


Fig. 3. Orthographic projection of the boundaries of the two retinal fields around the head of an animal while the eyes are in a resting position.

(A) American tree sparrow, (B) chipping sparrow, (C) dark-eyed junco, (D) Eastern towhee, (E) field sparrow, (F) song sparrow and (G) white-throated sparrow. Values are averaged across all individuals measured per species. A latitude and longitude coordinate system was used with the head of the animal at the center of the globe. The grid is set at 20 deg intervals and the equator aligned vertically in the median sagittal plane (the horizontal plane, 90–270 deg). The projections of the pecten produce a blind spot in the upper, frontal field. Projections of the bill tips are presented for orientation purposes.

Visual coverage and visual acuity

We found no significant relationship between visual acuity and the width of the cyclopean field (i.e. lateral plus binocular fields) at the horizontal plane with the eyes at ($F_{2,7}=2.50$, $P=0.151$, $R^2=0.26$, coefficient 2.93 ± 1.85 , $\lambda=0.73$). We decided to further assess this relationship but considering each component of the cyclopean field separately (binocular and lateral fields) because of the significant interspecific differences found above in the width of the binocular field.

Visual acuity was significantly and negatively associated with the width of the binocular field at the horizontal plane with the eyes at rest ($F_{2,7}=8.95$, $P=0.012$, $R^2=0.56$, coefficient -3.53 ± 1.18 , $\lambda=0$). Additionally, visual acuity was significantly and positively associated with width of the lateral field at the horizontal plane with the eyes at rest ($F_{2,7}=6.82$, $P=0.023$, $R^2=0.49$, coefficient 3.43 ± 1.32 , $\lambda=0$). Species with higher visual acuity tended to have narrower binocular fields (Fig. 4D), but wider lateral areas (Fig. 4E).

Retinal configuration and degree of eye movements

We found that the mean slope of the change in ganglion cell density from the retinal periphery to the fovea was positively associated with the degree of eye movements across all elevations ($F_{2,7}=6.48$, $P=0.026$, $R^2=0.48$, coefficient 5.75 ± 2.26 , $\lambda=0$). Therefore, species with steeper cell density profiles tended to have a larger degree of eye movement (Fig. 4F).

DISCUSSION

Emberizid sparrows show some convergence in some visual traits identified previously in other Passeriformes that detect and consume

their prey at close distances: (1) a single retinal center of acute vision (fovea) in each eye with fronto-lateral projection into the lateral field; (2) wide binocular visual fields; (3) bills projecting towards the binocular field with the eyes at rest; and (4) large degrees of eye movement. However, our results also show that emberizid sparrows have an interesting visual field specialization: when they converge their eyes to widen their binocular fields, the bills of most of the studied species intrude into the area of binocular overlap. Functionally, this means that these sparrows would be able to see their bill tips. This is contrary to the binocular field configuration proposed for birds with ballistic pecking towards seeds (Martin, 2014), like these emberizid sparrows during the winter. The implication is that sparrows have the ability to modify their visual field configuration through eye movements to visually inspect the prey items held between their mandibles. This is characteristic of a few bird species that use their bills for precision-grasping (e.g. European starlings *Sturnus vulgaris*, Martin, 1986; white-breasted nuthatches *Sitta carolinensis*, Moore et al., 2013; Eastern meadowlark *Sterna magna*, Tyrrell et al., 2013). For emberizid sparrows, visualizing the bill tip may become particularly relevant during the breeding season when their diet shifts strongly towards catching insects, hence identifying prey (type, size, etc.) may optimize their parental investment. This finding emphasizes the functional relevance (and flexibility) of the Passeriform binocular field for foraging purposes.

Interestingly, we found a relatively large degree of inter-specific variability in several visual traits in emberizid sparrows despite the fact that they are closely related phylogenetically (Carson and Spicer, 2003). Associating this between-species variation in visual traits

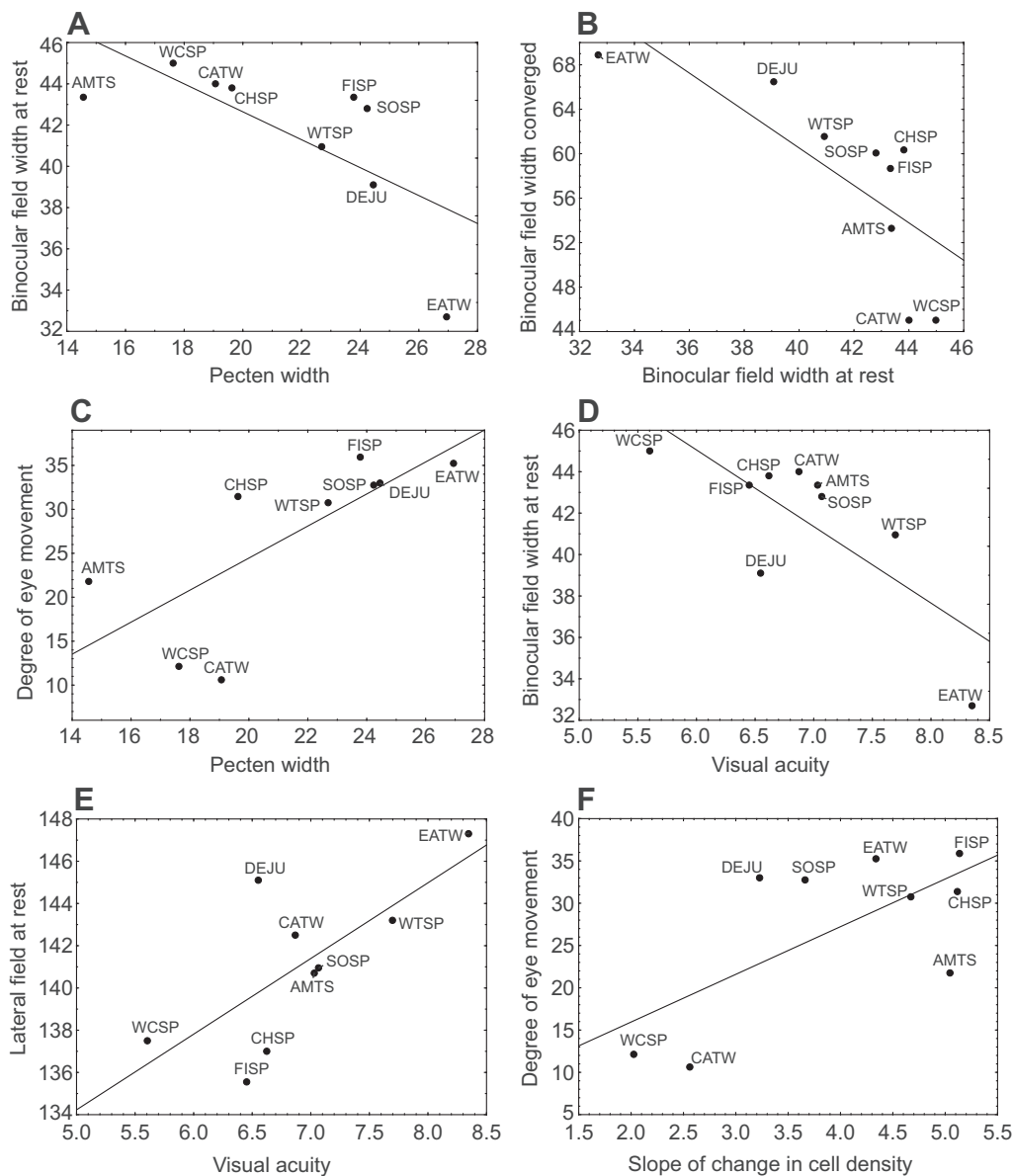


Fig. 4. Scatterplots showing the relationships (raw species data) between different visual traits in nine emberizid sparrows.

(A) binocular field width at the horizontal plane with eyes at rest (deg) vs pecten width across elevations (deg); (B) binocular field width (deg) at the horizontal plane with the eyes converged versus binocular field width at the horizontal plane with eyes at rest (deg); (C) degree of eye movement across elevations (deg) vs pecten width across elevations (deg); (D) binocular field width at the horizontal plane with eyes at rest (deg) vs visual acuity (cycles/degree); (E) lateral field width at the horizontal plane with eyes at rest (deg) vs visual acuity (cycles/deg); and (F) degree of eye movement across elevations (deg) vs averaged slope of change in cell density across the retina (considering the temporal, frontal, ventral, dorsal retinal areas). Abbreviations as in Fig. 2.

with that in behavior could be challenging given the overlap in foraging and anti-predator strategies in these species (supplementary material Table S1), although we can highlight some patterns. Species that have the highest visual acuity (relative to body mass) most commonly prey on flying insects (Eastern towhee, white-throated sparrow and American tree sparrow; supplementary material Table S1). Additionally, species with relatively higher visual acuity (towhees and song sparrows) tend to be more territorial compared with species with relatively lower acuity (hence, with lower probabilities of detecting predators from far away; Tisdale and Fernández-Juricic, 2009), which tend to flock more (field sparrows, dark-eyed juncos; Goodson et al., 2012). The implication is that the benefits of flocking (dilution and collective detection effects; Krause and Ruxton, 2002) might compensate for some sensory constraints.

The size of the pecten varied significantly between sparrows. Species with larger pectens could be constrained in terms of visual coverage as a result of the larger blind spot in the upper part of their visual fields. Furthermore, the size of the pecten may limit the spatial extent of binocular vision: species with larger pectens have narrower binocular fields with the eyes at rest. Our findings suggest

that this sensory challenge may be solved by moving the eyes: species with larger pectens have a larger degree of eye movement that allows them to converge their eyes and widen their binocular fields. On the other end of the continuum, species with narrower pectens have wider binocular fields with the eyes at rest and a lower degree of eye movement, probably because of the lower need to converge their eyes. Consequently, maintaining a relatively large degree of binocular vision (between approximately 45 deg and 65 deg) may have important functional consequences for emberizid sparrows in terms of finding and manipulating food items.

Most of the studied sparrows have temporally placed foveae that project into the lateral fields near the edges with the binocular field (but not intruding into the binocular field itself with the eyes at rest). From a foraging perspective, this visual configuration would allow emberizid sparrows to explore the substrate using (1) binocular vision (subtended by the peripheral areas of the retina) when the bill is perpendicular to the substrate, and (2) the foveae with the eyes converged by moving the bill just a few degrees to the sides (Fig. 5). Combining the inputs of the wide binocular field with those of the foveae within a limited range of head movements could actually

shorten the processing time of the binocular and monocular visual inputs, ultimately enhancing food detection and handling. This may be in contrast to species with relatively narrower binocular fields and with more centrally placed centers of acute vision (hence projecting more laterally), which would need a wider range of head movements to visually explore the foraging substrate (i.e. from bill pointing directly to the substrate to bill pointing almost laterally to align the fovea with the substrate; Fig. 5). Additionally, while head-down, emberizid sparrows could diverge their eyes to project their foveae more laterally and increase the chances of detecting potential threats (e.g. conspecifics trying to displace individuals from a foraging patch, predators etc.) at further distances, given the higher visual acuity provided by the fovea.

The combination of monocular and binocular viewing has been proposed before in birds (Walls, 1942), particularly in species with two centers of acute vision per retina [two foveae, raptors (Frost et al., 1990); one fovea plus one area, pigeons (Bloch and Martinoya, 1983)]. However, emberizid sparrows have a single center of acute vision. Sparrows may then maximize visual sampling at close distances to the substrate with a wide binocular field and closely spaced centers of acute vision. Although the perception benefits of using the foveae are clear (e.g. higher quality visual information), the contribution of the binocular field in emberizid sparrows is still unclear given that it is subtended by peripheral areas of the retina with lower density of ganglion cells and photoreceptors. One possibility is that the summation of the right and left visual inputs enhances contrast discrimination when the bill is perpendicular to the substrate (Heesy, 2009), which could increase the ability of an individual to resolve food items from the background. Another possibility is that the binocular overlap improves the ability to guide spatially and temporally the bill into the substrate to increase the precision to grab a food item (Martin, 2009). The implication is that the temporal part of the retina subtending the binocular field needs to be studied more in emberizid sparrows (e.g. relative density of different photoreceptors involved in chromatic and achromatic contrast, ratio of cones to ganglion cells, etc.) to understand how these species juggle their visual attention among different types of visual inputs (binocular, monocular) given their single center of acute vision.

Along a different visual axis, we found that emberizid sparrows with narrower binocular fields with the eyes at rest also have higher visual acuity and wider lateral visual fields. This is contrary to the

idea accepted in the vertebrate literature that species with relatively lower visual acuity should have wider visual coverage (Hughes, 1977). One possibility is that higher acuity and wider lateral visual coverage may compensate for the wider blind spots in the visual field (i.e. pectens) of these species (see above). Additionally, visual acuity is positively associated with body mass in birds (Kiltie, 2000). Given their body mass range, larger emberizid sparrows may be subject to higher predation rates from aerial predators (e.g. Gotmark and Post, 1996; Roth et al., 2006) and thus may benefit from enhanced predator detection from further away and from wider areas of visual coverage around their heads. However, the larger species (Eastern towhee, California towhee and white-throated sparrow) tend to forage in more covered or dense habitats (supplementary material Table S1), which would help hide them from aerial attacks.

A large degree of eye movement appears to be a common characteristic of Passeriformes (e.g. Fernández-Juricic et al., 2008). We found that at least part of the variation in eye movement in emberizid sparrows may be accounted for by the configuration of the retina. Cell density profiles provide a proxy of the variation in visual resolution across the retina (hence, across the visual field). In general, ganglion cell density is the highest around the fovea and decreases towards the retinal periphery (Fig. 1). Yet this decrease in cell density could be more or less pronounced, leading to a higher or lower difference in cell density between the fovea and the retinal periphery, respectively (Moore et al., 2012). Our results show that species with greater difference in cell density between the fovea and retinal periphery (i.e. higher slopes) have a greater degree of eye movement. Species with higher cell density difference have been hypothesized to rely more on the center of acute vision for gathering high quality information because of the relatively lower levels of visual resolution elsewhere in the retina (Dolan and Fernández-Juricic, 2010), which would lead to a greater need to move the eyes to get snapshots of high visual resolution from different parts of the visual environment (Fernández-Juricic et al., 2011a). Species with a lower cell density difference may have a proportionally greater area of the retina with high visual resolution and thus the need for eye movement may be reduced (Fernández-Juricic et al., 2011a). Future research should determine whether the covariation between retinal configuration and eye movement could affect the prevalence of different types of visual attention mechanisms, such as overt (centered around the fovea) and covert (centered around the retinal periphery) attention (Bisley, 2011).

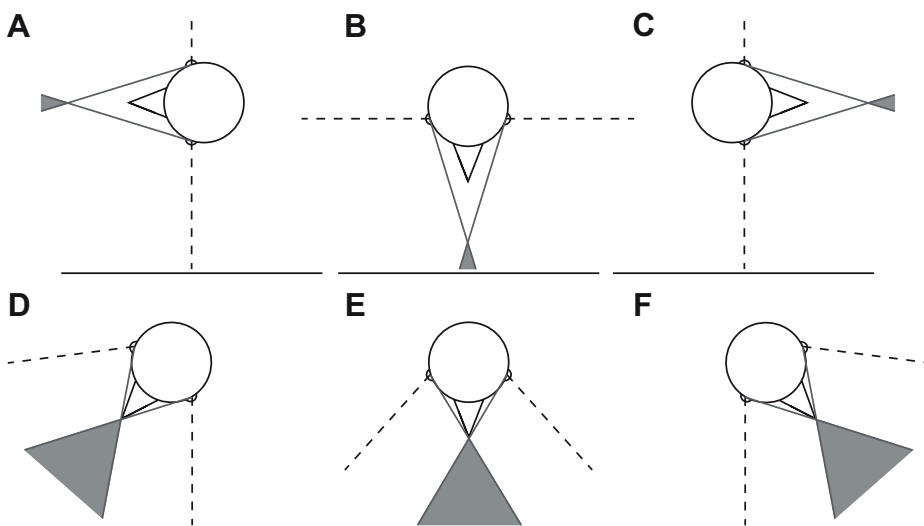


Fig. 5. Range of head movements in species with different fovea projections. A hypothetical bird with a narrow binocular field and laterally projecting foveae inspecting a foraging substrate with the (A) left fovea, (B) binocular field and (C) right fovea. A white-throated sparrow inspecting the foraging substrate with its eyes in a converged position with (D) left fovea, (E) binocular field and (F) right fovea. The hypothetical bird would rotate its head 90 deg to switch from viewing with the fovea to the binocular field (A to B) and a total of 180 deg to switch from one fovea to the other (A to C). The white-throated sparrow, on the other hand, would only rotate its head 40 deg to switch between the fovea and the binocular field (D to E) and 80 deg to switch between foveae. Dotted lines represent the projections of the foveae from the right and left eyes. The shaded region represents the binocular field and the solid line at the bottom of the figure represents the foraging substrate.

We also found that some proposed associations between visual traits were not as strong in emberizid sparrows as in non-Passeriformes. For example, we did not find a relationship between eye size and blind area width, as predicted by the glare hypothesis (Martin and Katzir, 2000). This could be related to our low sample size (i.e. nine species). Alternatively, the eye size range of emberizid sparrows may not be as strongly affected by imaging the sun as those species with much larger eyes (Martin, 2014), which generally exhibit sunshade structures such as eye lashes (Martin and Coetzee, 2004). This is not to say that glare does not affect relatively small species (e.g. Fernández-Juricic et al., 2012), but emberizid sparrow may use behavioral strategies to minimize these effects, such as avoiding sunlit patches, decreasing head-up vigilance bouts and aligning the pecten with the sun (Fernández-Juricic and Tran, 2007; van den Hout and Martin, 2011).

Emberizid sparrows visual configuration is considerably different from those reported previously in other groups of birds, such as sit-and-wait foragers (two centers of acute vision, high visual acuity, narrow binocular fields, wide blind areas, low eye movement amplitude; Coimbra et al., 2006, 2009; Jones et al., 2007; O'Rourke et al., 2010a,b) and tactile foragers (low visual acuity, narrow binocular fields, bill does not project into binocular field; Martin, 1994; Martin et al., 2007). Consequently, we propose that the visual system of emberizid passive prey foragers evolved to meet multiple sensory demands for foraging and predator detection purposes, particularly because their small eye sizes could limit their overall visual acuity compared with larger species.

MATERIALS AND METHODS

All sparrows used in this study were captured in Tippecanoe County, IN, USA. All capture, handling and experimental procedures were approved by the Purdue Animal Care and Use Committee (protocol 09-018). Birds were housed indoors with 1–3 individuals of the same species per (0.9×0.7×0.6 m) cage and kept on a 14 h:10 h light:dark cycle at approximately 23°C. Animals were provided food (millet) and water *ad libitum*. We used 8 American tree sparrows, 5 Chipping sparrows, 13 dark-eyed juncos, 3 Eastern towhees, 7 field sparrows, 9 song sparrows and 11 white-throated sparrows for visual field and degree of eye movement measurements, of which 3–5 individuals from each species were used for retina extraction to measure eye size, retinal ganglion cell density and to estimate the position of the center of acute vision.

Eye size, retinal ganglion cell density and visual acuity

Immediately after death, we removed the eyes and measured eye axial length from the anterior portion of the cornea to the most posterior part of the eye using digital calipers (0.01 mm accuracy). We then hemisected the eye at the *ora serrata* and removed all vitreous humor using forceps and spring scissors. Orientation of the eye was maintained throughout by the position of the pecten (Meyer, 1977) in relation to the bill. After extraction of the retina, it was whole-mounted and stained with Cresyl Violet for visualization of ganglion cells and counting, following the whole-mount technique described in detail in Ullmann et al. (2012). A thorough description of our methods to process the retinal tissue and count retinal ganglion cells (using standard cytological criteria) has been recently published in Baumhardt et al. (2014). We chose to stain ganglion cells because they have been proposed to be the information bottlenecks from the retina to the visual centers of the brain (Collin, 1999) and therefore have an important role in visual acuity (McIlwain, 1996). Details on the counting of retinal ganglion cells are provided below.

We built topographical representations of the cell densities across the retina (i.e. retinal topographic maps) following Stone (1981) and Ullmann et al. (2012). Ganglion cell density values obtained from each counting frame were then entered into a blank map showing the retinal outline and the sampling grid. We then created isodensity lines by hand, separating grid boxes into different cell density ranges (Moroney and Pettigrew, 1987;

Wathey and Pettigrew, 1989). The final topographic maps were developed using Adobe Illustrator CS5.

We assumed similar eye shapes and optical properties across species (Martin, 1993) because all our study species are diurnal (supplementary material Table S1). We then used the sampling theorem to obtain a morphological estimate of spatial resolving power (i.e. a proxy of visual acuity or visual resolution) using eye size and retinal ganglion cell density (Hughes, 1977). First, we multiplied eye axial length by 0.60 (following Hughes, 1977; Martin, 1993) as an estimate of posterior nodal distance (PND; length from the posterior nodal point of the eye to the photoreceptor layer; Vakkur et al., 1963). We then calculated the retinal magnification factor (RMF, the linear distance on the retina subtending 1 deg of visual space; Pettigrew et al., 1988) by using the following equation: $RMF = 2\pi PND / 360$. We then estimated spatial resolving power (in cycles per degree) to be the highest spatial

frequency that can be detected ($F_n = \frac{RMF}{2} \sqrt{\frac{2D}{\sqrt{3}}}$; where D is the averaged

retinal ganglion cell density throughout the retina (Williams and Coletta, 1987). The distance at which an object occupies the same angle of retinal space as one cycle at the threshold of visual acuity can be considered the theoretical maximum distance that an animal could detect that object under optimal ambient light conditions. We calculated the distance (d) at which each sparrow species could detect objects the size of a Cooper's hawk (*Accipiter cooperii*) wingspan (0.76 m; http://www.allaboutbirds.org/guide/Coopers_Hawk/lifehistory) and sharp-shinned hawk (*Accipiter striatus*) wingspan (0.49 m; http://www.allaboutbirds.org/guide/sharp-shinned_hawk/lifehistory) using: $d = r / \tan \frac{\alpha}{2}$, where r is the radius of the object (wingspan) and α is the inverse of visual acuity. We assumed that the whole diameter of the wingspan equaled one cycle.

Counting of retinal ganglion cells

We used an Olympus BX51 microscope to examine the retina. Using Stereo Investigator (ver. 9.13; MBF Bioscience), we first traced the perimeter of the retina with the SRS Image Series Acquire module. This module uses a fractionator approach to randomly and systematically place a grid onto the traced retina. We used on average between 407 and 413 grid sites per species (see supplementary material Table S3), but we counted ganglion cells on fewer sites [between 357 and 398 per species (supplementary material Table S3)] because some counting frames were outside of the retina, some retinal spots were out of focus or had tears. Each grid site contained a counting frame in the upper left hand corner that was 50×50 μm. The following parameters were then estimated: asf (the ratio of the area of the counting frame to the area of the grid), $\sum Q^-$ (sum of the total number of retinal ganglion cells counted) and the total number of ganglion cells in the retina (supplementary material Table S3). At each counting frame, we focused at ×1000 total power on the plane that provided the highest resolution and contrast to enable identification of ganglion cells. We then took a photograph of the focused counting frame with an Olympus S97809 microscope camera. Each photograph was captured and saved using Snagit (www.techsmith.com/Snagit). We counted the retinal ganglion cells in each of the images using ImageJ (<http://imagej.nih.gov/ij/>).

We differentiated retinal ganglion cells from amacrine and glial cells based upon cell shape, relatively soma size, Nissl accumulation in the cytoplasm and nuclear staining using standard cytological criteria (Hughes, 1977; Freeman and Tancred, 1978; Ehrlich, 1981; Stone, 1981; Mitkus et al., 2014). We differentiated retinal ganglion cells from all other cell types throughout the entire retina, however nearly every cell within the high ganglion cell density regions was counted because the non-ganglion cell population declines below 1% of the total cell count (Ehrlich, 1981). We discuss this approach to differentiating ganglion cells in detail in Fernández-Juricic et al. (2011b) and Baumhardt et al. (2014).

To correct for shrinkage of the retina during processing, we photographed the retina with a Panasonic Lumix FZ28 digital camera before and after the staining procedure, with an image area of 0.01 mm². ImageJ was then used to measure the area of the retina before and after staining. The amount of shrinkage in each picture was calculated by multiplying the area of the picture by the difference in retinal area before

and after the staining procedure. The average (\pm s.e.) shrinkage for all retinas was 0.04 ± 0.01 .

Cell density profile and position of the center of acute vision

We measured the position of the center of acute vision following a Cartesian coordinate system in relation to the center of the retina, where positive x -values indicate nasal and negative x -values indicate temporal and positive y -values indicate dorsal and negative y -values indicate ventral positioning (details in Moore et al., 2012). Ganglion cell density gradients were measured by establishing sampling transects across the nasal, temporal, dorsal and ventral retinal axes, centered on the center of acute vision (see Moore et al., 2012). The average density of retinal ganglion cells was recorded at each sampling point by establishing which cell density range each sampling point fell into. These sampling points were then plotted linearly and fit with a trend line from which the slope was calculated for use as an approximation for the change in RGC density from the retinal periphery to the center of acute vision (Moore et al., 2012). Variations in ganglion cell density across the retina provide an estimate of how visual acuity changes between the retinal periphery and the center of acute vision (i.e. the higher cell density, the higher the acuity or visual resolution).

To determine the angular projection of the center of acute vision into visual space, we converted the Cartesian coordinates into angular coordinates by multiplying the Cartesian value by the half width of the visual field of a single eye. We then aligned the center of the retina with the center of the single eye visual field and expressed the center of acute vision projection as the angular offset from standard positions in the x (line perpendicular to the beak axis) and y (parallel to the ground) dimensions. This method assumes that regions across the retina of equal size subtend equal angles of visual space, which appears to be the case in birds (Holden et al., 1987).

Visual field configuration and degree of eye movement

We used a visual field apparatus and an ophthalmoscope to measure the visual fields (see Martin, 1984 for a thorough description). Following methods described in detail in Moore et al. (2013), birds were placed in the visual field apparatus with their heads held stationary. The visual fields were measured using a polar coordinate system, such that the 90–270 deg plane was the horizontal plane (i.e. parallel to the ground); the 0 deg elevation lay directly above the head of each species, 90 deg in front and 270 deg behind (see Results). We measured with the ophthalmoscope the retinal boundaries at every 10 deg elevation around the head (± 0.5 deg), which was then mathematically corrected for close viewing following Martin (1984). We measured as many elevations around the subject as possible unless our view was blocked by its body or the apparatus. Overlapping retinal projections from both eyes at a given elevation represent the binocular field, whereas the lack of any retinal projection into an area represents the blind area. Using these two values, we calculated the size of the lateral fields as: $[360 - (\text{mean blind field} + \text{mean binocular field})/2]$ (Fernández-Juricic et al., 2008). With the eyes at rest, we also measured the size of the blind spot in the dorso-frontal part of the visual field caused by the projection of the pecten.

We measured the visual field configuration not only when the eyes were at rest, but also when (1) the eyes were converged, and (2) the eyes were diverged. We motivated the animals to move their eyes with sounds (e.g. keys) or a small flashlight. The degree of eye movement in a particular direction (elevation) was calculated by the difference between the converged and diverged values. Binocular field, blind area and the lateral fields were calculated in the same manner as explained before for converged and diverged eye positions.

Bill size

We measured bill length (posterior nostril to tip of the bill), bill width (horizontal thickness at the anterior edge of the nostrils) and bill depth (vertical thickness at the anterior edge of the nostrils) following Willson (1971). Measurements were taken on 10 American tree sparrows, 16 chipping sparrows, 19 dark-eyed juncos, 24 Eastern towhees, 9 field sparrows, 6 song sparrows, 6 white-throated sparrows, 9 California towhees

and 11 white-crowned sparrows at the Field Museum, Chicago, IL and at Purdue University Department of Forestry and Natural Resources, West Lafayette, IN. Measurements are presented in supplementary material Table S2.

Bill length ($F_{8,101}=157.58$, $P<0.001$), width ($F_{8,101}=61.85$, $P<0.001$) and depth ($F_{8,101}=112.87$, $P<0.001$) varied significantly among the nine species of emberizid sparrows (supplementary material Table S2). Using these three variables, we ran a Principal Component Analysis that produced a single factor (hereafter, bill size; Eigenvalue=2.92) that accounted for 97.41% of the variability in the data. Bill length (factor score=−0.990), bill depth (factor score=−0.988) and bill width (factor score=−0.983) were negatively correlated with PC1 so that smaller values indicated larger bills. Bill size increased in the following order: chipping sparrow, field sparrow, dark-eyed junco, American tree sparrow, white-crowned sparrow, white-throated sparrow, song sparrow, Eastern towhee and California towhee (supplementary material Table S2). Bill size was significantly correlated with body mass ($R^2=−0.91$, $P<0.001$), such that larger species had larger bills.

Statistical analysis

We first established the degree of between-species variability on the seven sparrow species whose visual traits are described for the first time here. We ran general linear models with Statistica 10 (Tulsa, OK) to determine between-species differences in bill length, width and depth, eye axial length and the slopes of cell density change from the retinal periphery to the center of acute vision. After comparing eye axial length between species, we ran another general linear model considering the residuals of the regression between (\log_{10}) axial length and (\log_{10}) body mass to ascertain the variation in eye size relative to body mass between species.

We ran general linear mixed models in SAS 9.2 (Cary, NC) to determine between-species differences in overall (i.e. whole retina) and highest (i.e. around center of acute vision) ganglion cell density, width of the binocular field, blind area and pecten, and the degree of eye movements. Individual identity was included as a within-subject factor and species and elevation as the between-subject factors in all these models. We only used elevations around the head from which we had data on a positive (binocular area) or negative (blind area) overlap between the eyes. Therefore, the reported means did not include values from those elevations where we could not record data (see above). Throughout, we present least square means \pm s.e.

In testing the specific predictions laid out in the Introduction, we established associations between different visual traits using a single value (i.e. least squares mean) for each species. We accounted for the shared evolutionary history of these species by using phylogenetic generalized least-squares models (PGLS, Pagel, 1999; Nunn, 2011). PGLS models calculate using a maximum-likelihood procedure the parameter lambda (λ), which estimates the amount of phylogenetic signal in the model: $\lambda=0$ indicates that the residual error is completely independent of phylogeny, whereas $\lambda=1$ indicates that the residual error varies according to a Brownian motion model of evolution (i.e. trait similarity is lower with increasing phylogenetic distance).

We conducted all PGLS analyses using the Caper package (Orme et al., 2011) in R (R Development Core Team, 2010). We corroborated that our results met the model assumptions by visually inspecting the distribution of residuals and the fitted versus the residual values. We also checked for outliers (samples with values >3 or <-3 , Yan and Su, 2009) but did not detect any. For the PGLS analyses, we used a tree (supplementary material Fig. S7) based on the phylogenetic relationships of emberizid sparrows described in Carson and Spicer (2003). We also ran general linear models with these raw species data (i.e. species means without phylogenetic relatedness corrections) and got the same results (available upon request).

To test for the relationship between binocular field width and bill size, we used the width of the binocular field at the plane of the bill (90 deg) with the eyes at rest and with the eyes converged as this is the elevation involved in food searching. Bill size was the Principal Component Analysis factor that included bill length, width and depth (see supplementary material Table S2). We tested for the relationships between binocular field and pecten size by using the binocular field values at the plane of the bill (90 deg) with the eyes at rest and pecten width across all elevations. The hypothesis behind this prediction assumes that species with wide binocular fields with the eyes at

rest would also have wide binocular fields with the eyes converged, which we also tested using binocular field values at the plane of the bill (90 deg). To test the relationship between degree of eye movement and pecten width, we used values across all recorded elevations as the presence of the pecten blind spot can influence eye movement across the whole visual field. To test the relationship between blind area and eye size, and pecten width and eye size, we used the width of the blind area across all recorded elevations with the eyes at rest, the width of the pecten across all recorded elevations and the (\log_{10}) eye axial length as a proxy of eye size. To test the relationship between visual coverage and visual acuity, we calculated the width of the cyclopean field (combination of binocular and lateral fields) with the eyes at rest by subtracting the total amount of blind area from 360. We used the elevation around the plane of the bill for the cyclopean field because measurements from in front of the head and behind the head of a given plane must be present (e.g. 90 deg and 270 deg) to calculate the cyclopean field and only at the given elevations could both be calculated for every species. To test for the relationship between retinal configuration and degree of eye movements, we used the mean slope of the change in cell density between the retinal periphery and the center of acute vision (considering all directions: nasal, temporal, dorsal, ventral) and the average degree of eye movement across all elevations.

Acknowledgements

We thank the members of the Lucas and Bernal labs for constructive comments on an earlier draft of the manuscript.

Competing interests

The authors declare no competing or financial interests.

Author contributions

B.A.M., D.P. and L.P.T. conceived, designed and executed the study, interpreted the findings being published, and drafted and revised the manuscript. E.F.-J. conceived and designed the study, interpreted the findings being published, and drafted and revised the manuscript.

Funding

This study was funded by the National Science Foundation (IOS Award#1146986).

Supplementary material

Supplementary material available online at <http://jeb.biologists.org/lookup/suppl/doi:10.1242/jeb.108613/-/DC1>

References

- Barlow, H. B. and Ostwald, T. S. (1972). Pecten of the pigeon's eye as an intraocular eye shade. *Nature* **236**, 88-90.
- Baumhardt, P. E., Moore, B. A., Doppler, M. and Fernández-Juricic, E. (2014). Do American goldfinches see their world like passive prey foragers? A study on visual fields, retinal topography, and sensitivity of photoreceptors. *Brain Behav. Evol.* **83**, 181-198.
- Birkhead, T. (2012). *Bird Sense: What it's Like to be a Bird*. London: Bloomsbury.
- Birkhead, T., Wimpenny, J. and Montgomerie, B. (2014). *Ten Thousand Birds: Ornithology Since Darwin*. Princeton: Princeton University Press.
- Bisley, J. W. (2011). The neural basis of visual attention. *J. Physiol.* **589**, 49-57.
- Bloch, S. and Martinoya, C. (1983). Specialization of visual functions for the different retinal areas in the pigeon. In *Advances in Neuroethology* (ed. J. P. Ewert, R. R. Capranica and D. J. Ingle), pp. 359-368. New York: Plenum Press.
- Boughman, J. W. (2002). How sensory drive can promote speciation. *Trends Ecol. Evol.* **17**, 571-577.
- Carson, R. J. and Spicer, G. S. (2003). A phylogenetic analysis of the emberizid sparrows based on three mitochondrial genes. *Mol. Phylog. Evol.* **29**, 43-57.
- Coimbra, J. P., Marceliano, M. L. V., Andrade-da-Costa, B. L. D. and Yamada, E. S. (2006). The retina of tyrant flycatchers: topographic organization of neuronal density and size in the ganglion cell layer of the great kiskadee *Pitangus sulphuratus* and the rusty margined flycatcher *Myiozetetes cayanensis* (Aves: Tyrannidae). *Brain Behav. Evol.* **68**, 15-25.
- Coimbra, J. P., Trévia, N., Marcelliano, M. L. V., da Silveira Andrade-da-Costa, B. L., Picanco-Diniz, C. W. and Yamada, E. S. (2009). Number and distribution of neurons in the retinal ganglion cell layer in relation to foraging behaviors of tyrant flycatchers. *J. Comp. Neurol.* **514**, 66-73.
- Collin, S. P. (1999). Behavioural ecology and retinal cell topography. In *Adaptive Mechanisms in the Ecology of Vision* (ed. S. Archer, M.B. Djamgoz, E. Loew, J.C. Partridge and S. Vallergera), pp. 509-535. Dordrecht: Kluwer Academic Publishers.
- Crozier, W. J. and Wolf, E. (1944). Flicker response contours for the sparrow and the theory of the avian pecten. *J. Gen. Physiol.* **27**, 315-324.
- Cuthill, I. C. (2006). Color perception. In *Bird Coloration: Mechanisms and Measurements* (ed. G.E. Hill and K.J. McGraw), pp. 3-40. Cambridge: Harvard University Press.
- Dalton, B. E., Cronin, T. W., Marshall, N. J. and Carleton, K. L. (2010). The fish eye view: are cichlids conspicuous? *J. Exp. Biol.* **213**, 2243-2255.
- Dolan, T. and Fernández-Juricic, E. (2010). Retinal ganglion cell topography of five species of ground-foraging birds. *Brain Behav. Evol.* **75**, 111-121.
- Elphick, C., Dunning, J. B., Jr. and Sibley, D. A. (2001). *The Sibley Guide to Bird Life and Behavior*. New York: National Audubon Society, Alfred A. Knopf.
- Ehrlich, D. (1981). Regional specialization of the chick retina as revealed by the size and density of neurons in the ganglion cell layer. *J. Comp. Neurol.* **195**, 643-657.
- Fernández-Juricic, E. and Tran, E. (2007). Changes in vigilance and foraging behaviour with light intensity and their effects on food intake and predator detection in house finches. *Anim. Behav.* **74**, 1381-1390.
- Fernández-Juricic, E., Gall, M. D., Dolan, T., Tisdale, V. and Martin, G. R. (2008). The visual fields of two ground-foraging birds, House finches and house sparrows, allow for simultaneous foraging and anti-predator vigilance. *Ibis* **150**, 779-787.
- Fernández-Juricic, E., Gall, M. D., Dolan, T., O'Rourke, C., Thomas, S. and Lynch, J. R. (2011a). Visual systems and vigilance behaviour of two ground-foraging avian prey species: white-crowned sparrows and California towhees. *Anim. Behav.* **81**, 705-713.
- Fernández-Juricic, E., Moore, B. A., Doppler, M., Freeman, J., Blackwell, B. F., Lima, S. L. and DeVault, T. L. (2011b). Testing the terrain hypothesis: Canada geese see their world laterally and obliquely. *Brain Behav. Evol.* **77**, 147-158.
- Fernández-Juricic, E., Deisher, M., Stark, A. C. and Randolet, J. (2012). Predator detection is limited in microhabitats with high light intensity: an experiment with brown-headed cowbirds. *Ethology* **118**, 341-350.
- Freeman, B. and Tancred, E. (1978). The number and distribution of ganglion cells in the retina of the brush-tailed possum, *Trichosurus vulpecula*. *J. Comp. Neurol.* **177**, 557-567.
- Frost, B. J., Wise, L. Z., Morgan, B. and Bird, D. (1990). Retinotopic representation of the bifoveate eye of the kestrel (*Falco sparverius*) on the optic tectum. *Vis. Neurosci.* **5**, 231-239.
- Gall, M. D. and Fernández-Juricic, E. (2010). Visual fields, eye movements, and scanning behavior of a sit-and-wait predator, the Black Phoebe (*Sayornis nigricans*). *J. Comp. Physiol. A* **196**, 15-22.
- Goodson, J. L., Wilson, L. C. and Schrock, S. E. (2012). To flock or fight: neurochemical signatures of divergent life histories in sparrows. *Proc. Natl. Acad. Sci. USA* **109** Suppl. 1, 10685-10692.
- Gotmark, F. and Post, P. (1996). Prey selection by sparrowhawks, *Accipiter nisus*: relative predation risk for breeding passerine birds in relation to their size, ecology and behaviour. *Phil. Trans. Royal Soc. Lond. B* **351**, 1559-1577.
- Heesy, C. P. (2009). Seeing in stereo: the ecology and evolution of primate binocular vision and stereopsis. *Evol. Anthropol.* **18**, 21-35.
- Holden, A. L., Hayes, B. P. and Fitzke, F. W. (1987). Retinal magnification factor at the ora terminalis: a structural study of human and animal eyes. *Vision Res.* **27**, 1229-1235.
- Hughes, A. (1977). The topography of vision in mammals of contrasting life style: comparative optics and retinal organization. In *The Visual System in Vertebrates* (ed. F. Crescitelli), pp. 615-756. New York: Springer-Verlag.
- Inzunza, O., Bravo, H., Smith, R. L. and Angel, M. (1991). Topography and morphology of retinal ganglion cells in Falconiformes: a study on predatory and carrion-eating birds. *Anat. Rec.* **229**, 271-277.
- Jones, M. P., Pierce, K. E., Jr and Ward, D. (2007). Avian vision: a review of form and function with special consideration to birds of prey. *J. Exotic Pet. Med.* **16**, 69-87.
- Kiltie, R. A. (2000). Scaling of visual acuity with body size in mammals and birds. *Func. Ecol.* **14**, 226-234.
- Koch, D. D. (1989). Glare and contrast sensitivity testing in cataract patients. *J. Cataract Refract. Surg.* **15**, 158-164.
- Krause, J. and Ruxton, G. D. (2002). *Living in Groups*. Oxford: Oxford University Press.
- Lazareva, O. F., Shimizu, T. and Wasserman, E. A. (2012). *How Animals see the World: Comparative Behavior, Biology, and Evolution of Vision*. Oxford: Oxford University Press.
- Martin, G. R. (1984). The visual fields of the tawny owl, *Strix aluco* L. *Vision Res.* **24**, 1739-1751.
- Martin, G. R. (1986). The eye of a passeriform bird, the European starling (*Sturnus vulgaris*): eye movement amplitude, visual fields and schematic optics. *J. Comp. Physiol. A* **159**, 545-557.
- Martin, G. R. (1993). Producing the image. In *Vision, Brain and Behaviour in Birds*. (ed. H. P. Zeigler and H.-J. Bischof), pp. 5-24. Massachusetts: MIT press.
- Martin, G. R. (1994). Visual fields in woodcocks *Scolopax rusticola* (Scolopacidae; Charadriiformes). *J. Comp. Physiol. A* **174**, 787-793.
- Martin, G. R. (2007). Visual fields and their functions in birds. *J. Ornithol.* **148**, 547-562.
- Martin, G. R. (2009). What is binocular vision for? A birds' eye view. *J. Vision* **9**, 14.

- Martin, G. R.** (2012). Through birds' eyes: insights into avian sensory ecology. *J. Ornithol.* **153** Suppl. 1, 23-48.
- Martin, G. R.** (2014). The subtlety of simple eyes: the tuning of visual fields to perceptual challenges in birds. *Phil. Trans. R. Soc. B Biol. Sci.* **369**, 20130040.
- Martin, G. R. and Coetzee, H. C.** (2004). Visual fields in hornbills: precision-grasping and sunshades. *Ibis* **146**, 18-26.
- Martin, G. R. and Katzir, G.** (2000). Sun shades and eye size in birds. *Brain Behav. Evol.* **56**, 340-344.
- Martin, G. R. and Prince, P. A.** (2001). Visual fields and foraging in procellariiform seabirds: sensory aspects of dietary segregation. *Brain Behav. Evol.* **57**, 33-38.
- Martin, G. R., Jarrett, N. and Williams, M.** (2007). Visual fields in blue ducks *Hymenolaimus malacorhynchos* and pink-eared ducks *Malacorhynchus membranaceus*: visual and tactile foraging. *Ibis* **149**, 112-120.
- McIlwain, J. T.** (1996). *An Introduction to the Biology of Vision*. New York: Cambridge University Press.
- Meyer, D. B. C.** (1977). The avian eye and its adaptations. In *The Visual System of Vertebrates; Handbook of Sensory Physiology* (ed. F. Crescitelli), pp. 549-612. New York: Springer.
- Mitkus, M., Chaib, S., Lind, O. and Kelber, A.** (2014). Retinal ganglion cell topography and spatial resolution of two parrot species: budgerigar (*Melopsittacus undulatus*) and Bourke's parrot (*Neopsephotus bourkii*). *J. Comp. Physiol. A* **200**, 371-384.
- Moore, B. A., Kamilar, J. M., Collin, S. P., Bininda-Emonds, O. R. P., Dominy, N. J., Hall, M. I., Heesy, C. P., Johnsen, S., Lisney, T. J., Loew, E. R. et al.** (2012). A novel method for comparative analysis of retinal specialization traits from topographic maps. *J. Vision* **12**, 13.
- Moore, B. A., Doppler, M., Young, J. E. and Fernández-Juricic, E.** (2013). Interspecific differences in the visual system and scanning behavior of three forest passerines that form heterospecific flocks. *J. Comp. Physiol. A* **199**, 263-277.
- Moroney, M. K. and Pettigrew, J. D.** (1987). Some observations on the visual optics of kingfishers (Aves, Coraciiformes, Alcedinidae). *J. Comp. Physiol. A* **160**, 137-149.
- Nunn, C.** (2011). *The Comparative Approach in Evolutionary Anthropology and Biology*. Chicago: University of Chicago Press.
- Orme, C. D. L., Freckleton, R. P., Thomas, G. H., Petzoldt, T. and Fritz, S. A.** (2011). caper: Comparative Analyses of Phylogenetics and Evolution in R (<http://R-Forge.R-project.org/projects/caper/>).
- O'Rourke, C. T., Hall, M. I., Pitlik, T. and Fernández-Juricic, E.** (2010a). Hawk eyes I: diurnal raptors differ in visual fields and degree of eye movement. *PLoS ONE* **5**, e12802.
- O'Rourke, C. T., Pitlik, T., Hoover, M. and Fernández-Juricic, E.** (2010b). Hawk eyes II: diurnal raptors differ in head movement strategies when scanning from perches. *PLoS ONE* **5**, e12169.
- Pagel, M.** (1999). Inferring the historical patterns of biological evolution. *Nature* **401**, 877-884.
- Pettigrew, J. D., Dreher, B., Hopkins, C. S., McCall, M. J. and Brown, M.** (1988). Peak density and distribution of ganglion cells in the retinae of Microchiropteran bats: implications for visual acuity. *Brain Behav. Evol.* **32**, 39-56.
- Pettigrew, J. D., Wallman, J. and Wildsoet, C. F.** (1990). Saccadic oscillations facilitate ocular perfusion from the avian pecten. *Nature* **343**, 362-363.
- Reymond, L.** (1985). Spatial visual acuity of the eagle *Aquila audax*: a behavioural, optical and anatomical investigation. *Vision Res.* **25**, 1477-1491.
- Ricklefs, R. E.** (2012). Species richness and morphological diversity of passerine birds. *PNAS* **109**, 14482-14487.
- Roth, T. C., III, Lima, S. L. and Vetter, W. E.** (2006). Determinants of predation risk in small wintering birds: the hawk's perspective. *Behav. Ecol. Sociobiol.* **60**, 195-204.
- Safi, K. and Siemers, B. M.** (2010). Implications of sensory ecology for species coexistence: biased perception links predator diversity to prey size distribution. *Evol. Ecol.* **24**, 703-713.
- Seehausen, O., Terai, Y., Magalhaes, I. S., Carleton, K. L., Mrosso, H. D. J., Miyagi, R., van der Sluijs, I., Schneider, M. V., Maan, M. E., Tachida, H. et al.** (2008). Speciation through sensory drive in cichlid fish. *Nature* **455**, 620-626.
- Siemers, B. M. and Swift, S. M.** (2006). Differences in sensory ecology contribute to resource partitioning in the bats *Myotis bechsteinii* and *Myotis nattereri* (Chiroptera: Vespertilionidae). *Behav. Ecol. Sociobiol.* **59**, 373-380.
- Stone, J.** (1981). *The Wholemount Handbook. A Guide to the Preparation and Analysis of Retinal Wholemounts*. Sydney: Maitland Publishing.
- Tucker, R.** (1975). The surface of the pecten oculi in the pigeon. *Cell Tissue Res.* **157**, 457-465.
- Tucker, V. A.** (2000). The deep fovea, sideways vision and spiral flight paths in raptors. *J. Exp. Biol.* **203**, 3745-3754.
- Tyrrell, L. P., Moore, B. A., Loftis, C. and Fernández-Juricic, E.** (2013). Looking above the prairie: localized and upward acute vision in a native grassland bird. *Sci. Rep.* **3**, 3231.
- Tisdale, V. and Fernández-Juricic, E.** (2009). Vigilance and predator detection vary between avian species with different visual acuity and coverage. *Behav. Ecol.* **20**, 936-945.
- Ullmann, J. F. P., Moore, B. A., Temple, S., Fernández-Juricic, E. and Collin, S. P.** (2012). The retinal wholemount technique: a window to understanding the brain and behaviour. *Brain Behav. Evol.* **79**, 26-44.
- Vakkur, G. J., Bishop, P. O. and Kozak, W.** (1963). Visual optics in the cat, including posterior nodal distance and retinal landmarks. *Vision Res.* **3**, 289-314.
- Van der Hout, P. J. and Martin, G. R.** (2011). Extreme head-tilting in shore birds: predator detection and sun-avoidance. *Wader Study Group Bull.* **118**, 18-21.
- Walls, G. L.** (1942). *The Vertebrate Eye and its Adaptive Radiation*. Michigan: Cranbrook Institute of Science, Bloomfields Hills.
- Wathey, J. C. and Pettigrew, J. D.** (1989). Quantitative analysis of the retinal ganglion cell layer and optic nerve of the Barn Owl *Tyto alba*. *Brain Behav. Evol.* **33**, 279-292.
- Williams, D. R. and Coletta, N. J.** (1987). Cone spacing and the visual resolution limit. *J. Opt. Soc. Am. A* **4**, 1514-1523.
- Willson, M. F.** (1971). Seed selection in some North American finches. *Condor* **73**, 415-429.
- Wood, C.** (1917). *The Fundus Oculi of Birds, Especially as Viewed by the Ophthalmoscope; A Study in the Comparative Anatomy and Physiology*. Chicago: The Lakeside Press.
- Yan, X. and Su, X. G.** (2009). *Linear Regression Analysis: Theory and Computing*. London: World Scientific Publishing.